Post-synthesis annealing of MOF-5 remarkably enhances the framework structural stability and CO_2 uptake

Srinivas Gadipelli[a,]* and Zhengxiao Guo [a,]*

[a] Department of Chemistry, University College London, 20 Gordon Street, London, WC1H 0AJ, UK.

* E-mail: gsrinivasphys@gmail.com (S.G.); z.x.guo@ucl.ac.uk (Z.G.).

Experimental methods:

The MOF-5 sample was synthesized according to our earlier report [Ref. 22, and also see J. L. C. Rowsell, E. C. Spencer, J. Eckert, J. A. K. Howard, O. M. Yaghi, Gas adsorption sites in a large-pore metal-organic framework, *Science* **2005**, *309*, 1350]. In a typical synthesis, 6.3 g of zinc nitrate tetrahydrate (Merck) and 1.35 g of terephthalic acid (Aldrich) were dissolved in 300 ml of freshly distilled *N*,*N*-diethylformamide (Acros) in a 500 ml wide mouth glass jar (Fisherbrand) with screw tight cap. The tightly sealed glass jar left in an oven for 2 days at 100 °C. The crystals were washed with *N*,*N*-diethylformamide, and finally immersing in chloroform (Fisher). The exchange solvent was refreshed 5 times during 5 day period. Later the dry sample was obtained by evacuation under high vacuum while heating to 250 °C for 24 h. The sample was then stored in Ar-filled glove box for further use. The thermal annealing of MOF-5 at various temperatures was carried out in a horizontal tube furnace under continuous N_2 flow. Each time about 100 mg of MOF-5 sample was used in an alumina boat. Before being heated to the target temperature at 5 °C per minute, the furnace with the sample was purged with dry N_2 to make sure that no air or moisture residue remain that could degrade sample quality. After being cooled to room temperature, the sample was collected in a glass vial in ambient air. All samples for further characterizations were handled in Ar-filled glove box.

Characterization:

The combined thermogravimetric analysis (TGA, on Setsys from Setaram) and mass spectrometry (MS, on OmniStar from Pfeiffer Vacuum) were carried out on a dry sample under Ar flow after purging; after reaching the target temperature at a ramping rate of 5 °C per minute, the annealing step was carried out under an isothermal step for a suitable period of time, up to 50 h. The TGA mass-loss was recorded after background correction to empty alumina crucible. Powder X-ray diffraction (PXRD, on Stoe Stadi-P, Cu-K-alpha) was carried out by filling the sample in a (0.5-1.0) mm diameter glass capillary at ambient. Fourier-transform Infrared (FTIR, on Nicolet 6700 FTIR) data was obtained at room temperature by KBr pellet transmission method with background correction. X-ray Photoemission spectroscopy (XPS, on Al-K-alpha, Thermo Scientific) data were obtained on the samples depositing on carbon tape. The gas adsorption-desorption isotherm measurements at 77 K and 298 K using liquid nitrogen and water bath, respectively, up to 1 bar were carried out using a Quantachrome Autosorb-iQC. The specific surface area was measured from the 77 K N_2 desorption isotherm in the relative pressure range between 0.01 and 0.2, according to the Brunauer-Emmett-Teller (BET) method. DFT (density functional theory) method with slit/cylindrical pores was applied to desorption isotherm to obtain pore size distribution and cumulative pore volume. The CO_2 uptake isotherms at 0 °C, 25 °C and 50 °C (maintained by ice bath and precisely controlled temperature tube furnace) were measured on a PCTPro 2000. The isosteric heat of adsorption (Q_{st}) was determined from the isotherms measured at three different temperatures of 0 °C, 25 °C and 50 °C by applying the Clausius-Clapeyron relation. For this the experimental isotherm data were fitted with $3^{rd}/4^{th}$ order polynomical curves with 1000 data points. These fittings were used to record the corresponding pressures at discrete CO_2 uptakes levels. Thus at different CO_2 uptakes, the Q_{st} is determined from the slopes of the 'lnP vs 1/T' plots, using the relation $Q_{st} = -R \times (\text{slope})$. Where P is the equilibrium pressure, T is the isotherm temperature in K, and R is the universal gas constant. The CO_2 uptake cycling test was carried out on TGA under continuous CO_2 flow at ≈ 1 bar with the temperature swing between 31°C and 200 °C. The 10 °C per minute heating rate and TGA water cooling was applied for cycling. Each time a continuous 22 run segment was measured for 22 h and repeated it again on each sample. The sample was degassed at 150 °C overnight under dynamic vacuum before all the actual gas adsorption measurements.

Total pore volume is obtained at P/Po of ~ 0.99. Which is a simple relation, defined as, total pore volume = (N_2 adsorbed at 0.99 in cm^3/g) × (N_2 gas density at STP)/(N_2 liquid density at ~1 bar). This is equal to V_{ads} at (P/Po = 0.99) × 0.001547.

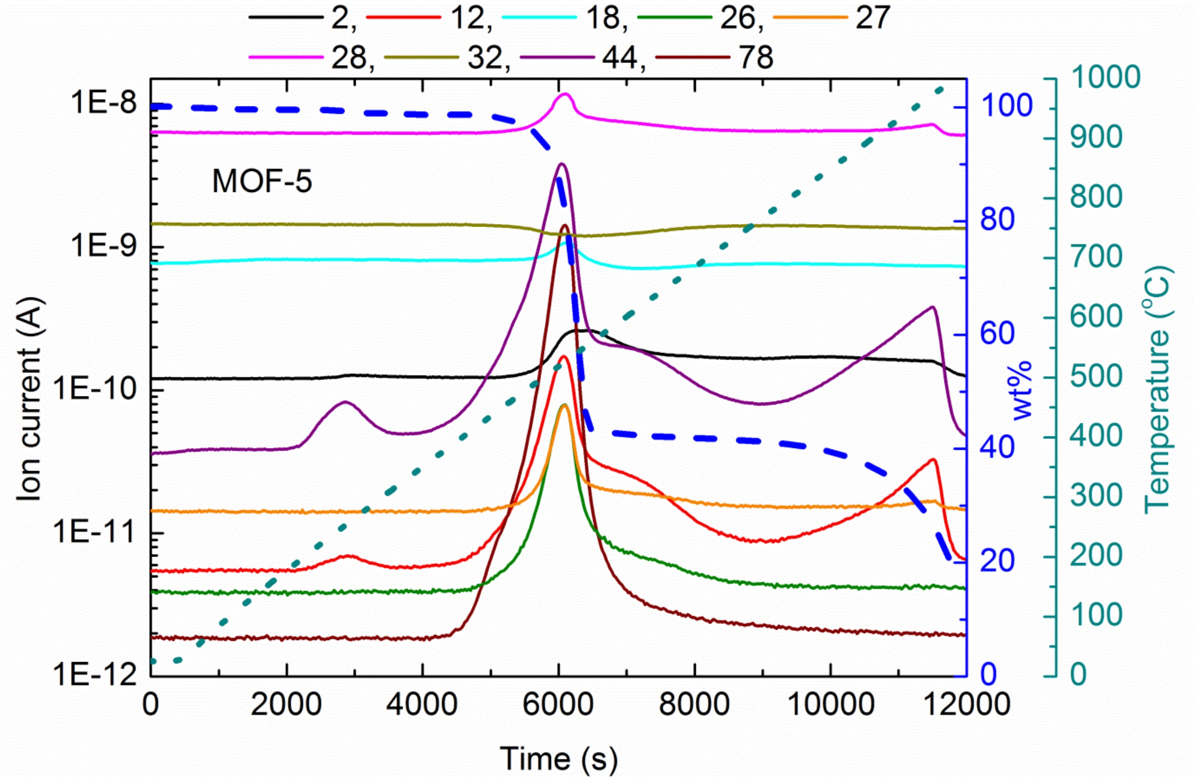

Figure S1. Combined TGA-MS analysis of dry MOF-5. TGA mass-loss (blue dashed curve) and ramping temperature (dark cyan dotted line) is on right y-axis and MS signal intensity on left y-axis are plotted against ramping time. The onset of decomposition around 500 °C is attributed primarily due to decomposition of framework bridged carboxylates in the form of CO_2 (atomic mass unit, amu signal at 44 and 12) and linker aromatic benzene (amu at 78) before the ring decomposition (amu at 26).

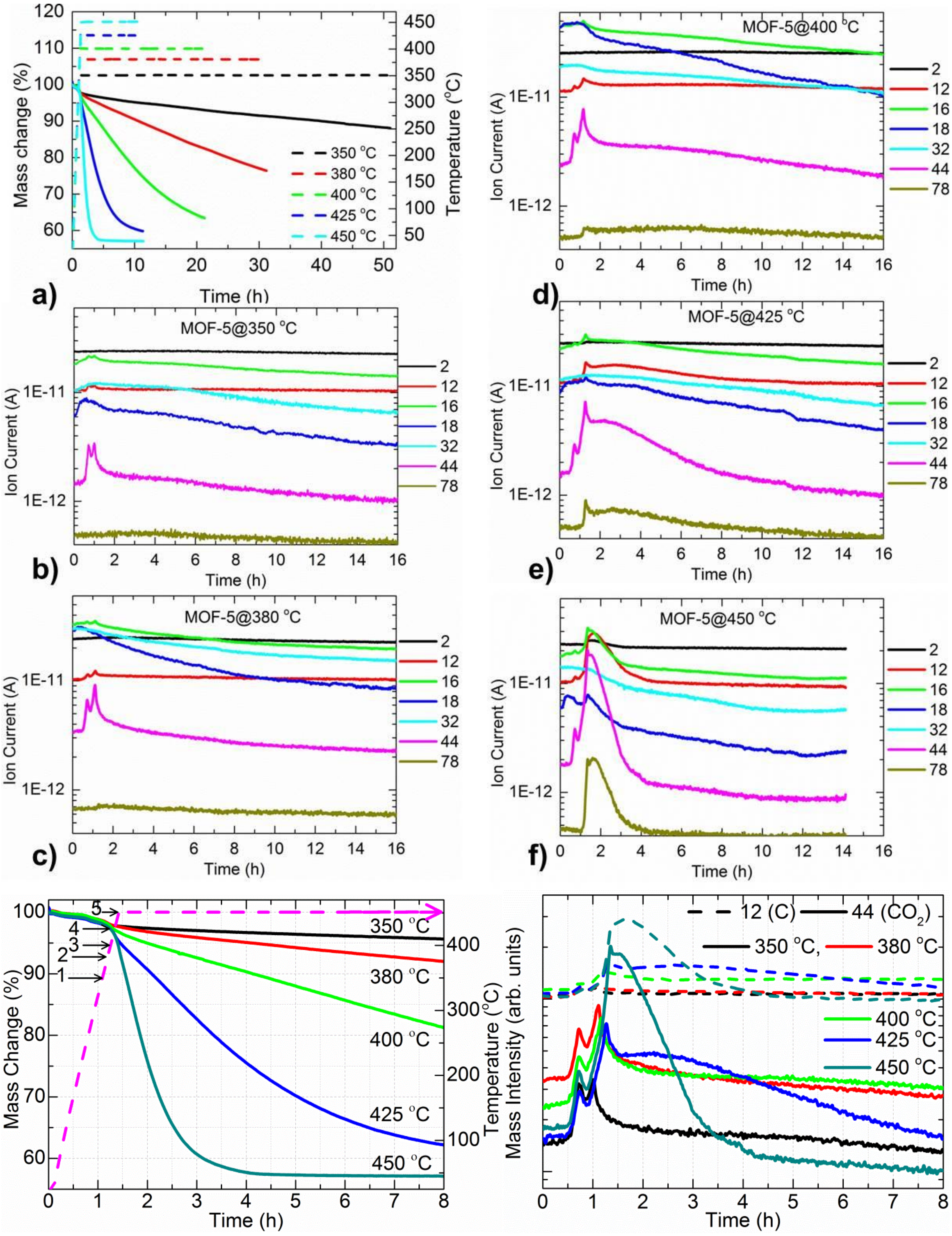

Figure S2. a). TGA plots for the prolonged isothermal tests at 350 °C (for 50 h), 380 °C (for 30 h), 400 °C (for 20 h), 425 °C (for 10 h) and 450 °C (for 10 h). The dashed and solid line data represent a sample temperature (right y-axis) and mass (left y-axis), respectively. b-f). Individually shows the MS plots for corresponding TGA isothermal tests. Different colour code MS curves represent the atomic mass unit numbers: 2-H_2, 12-C, 16-CH_4, 18-H_2O, 32-O_2, 44-CO_2, 78-C_6H_6. Clearly except CO_2 (see 44, 12 signals) there is no aromatic ring decomposition or linker evolution is detected between (350-380) °C, whereas at ≥ 400 °C linker benzene also evolves. Comparative TGA-MS plots are shown in bottom panel.

Table S1. TGA sample mass-loss against annealing temperature and time.

Sample	Mass-loss (wt%)
MOF-5	-
6h@350°C	4.2
24h@350°C	7.7
50h@350°C	11.8
1h@380°C	3.4
3h@380°C	5.0
6h@380°C	7.5
24h@380°C	21.0
1h@400°C	5.6
3h@400°C	10.3
6h@400°C	14.9
0h@450°C	5.5
1h@450°C	33.1
0h@500°C	10.5
1h@500°C	45.0

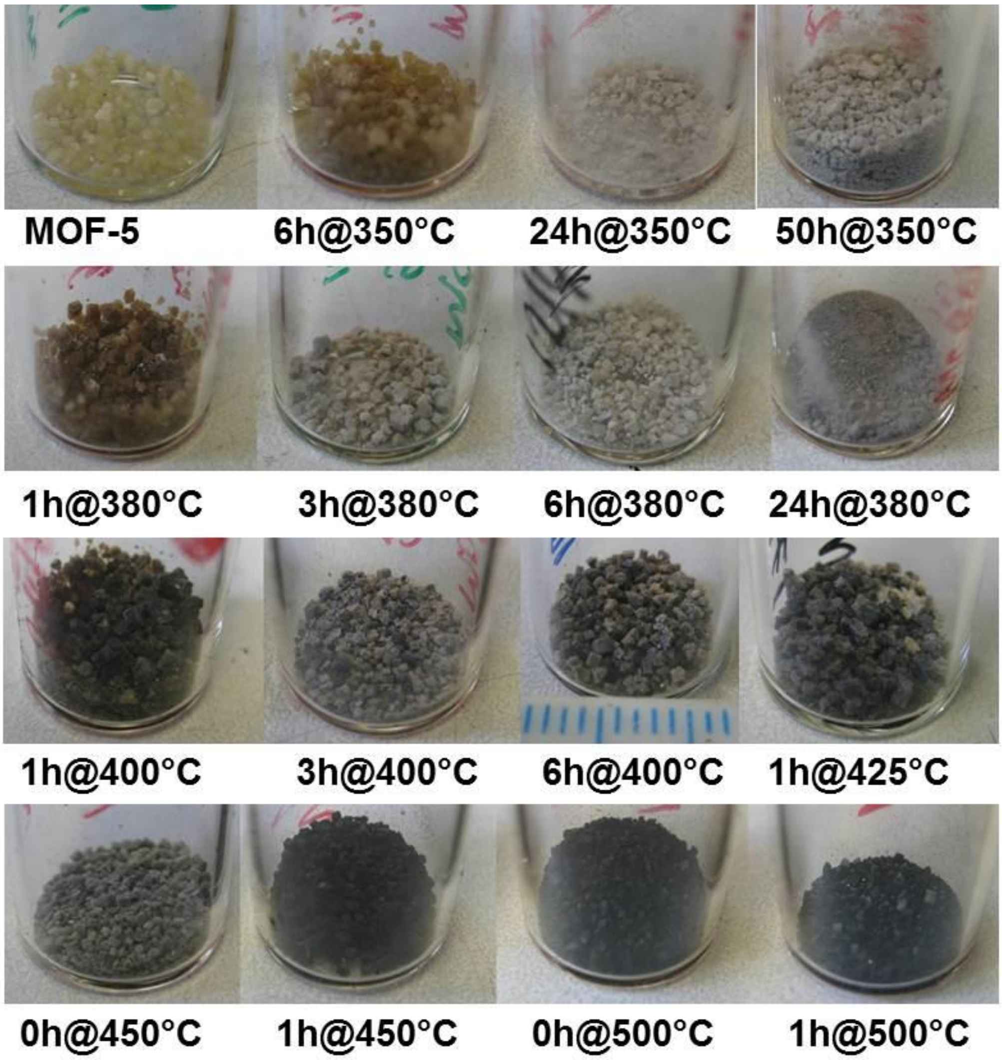

Figure S3a. Digital photographs of the MOF-5 and its annealed samples in glass vials, that were obtained at controlled times and temperatures as labelled below for each sample. The darkish at 400 °C could presumably be onset of carbonization before converting it to carbon (black) at 500 °C. The scale shows a millimetre sized MOF crystals [ref. 22].

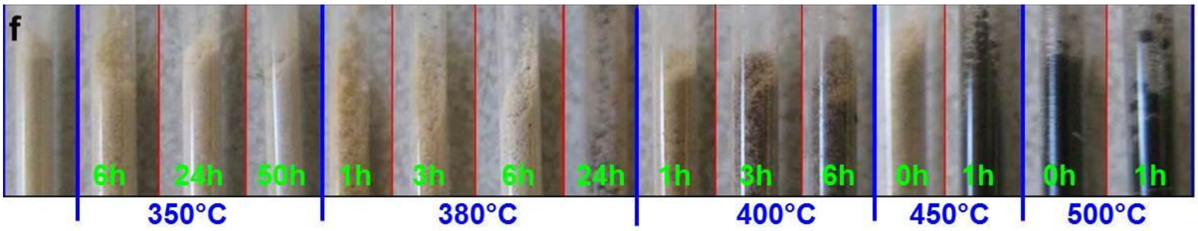

Figure S3b. Digital photographs of the powdered samples sealed in a glass capillary of (0.5-1) mm diameter used for X-ray diffraction; the sections from left to right are for MOF-5 and its annealed products with different annealing period.

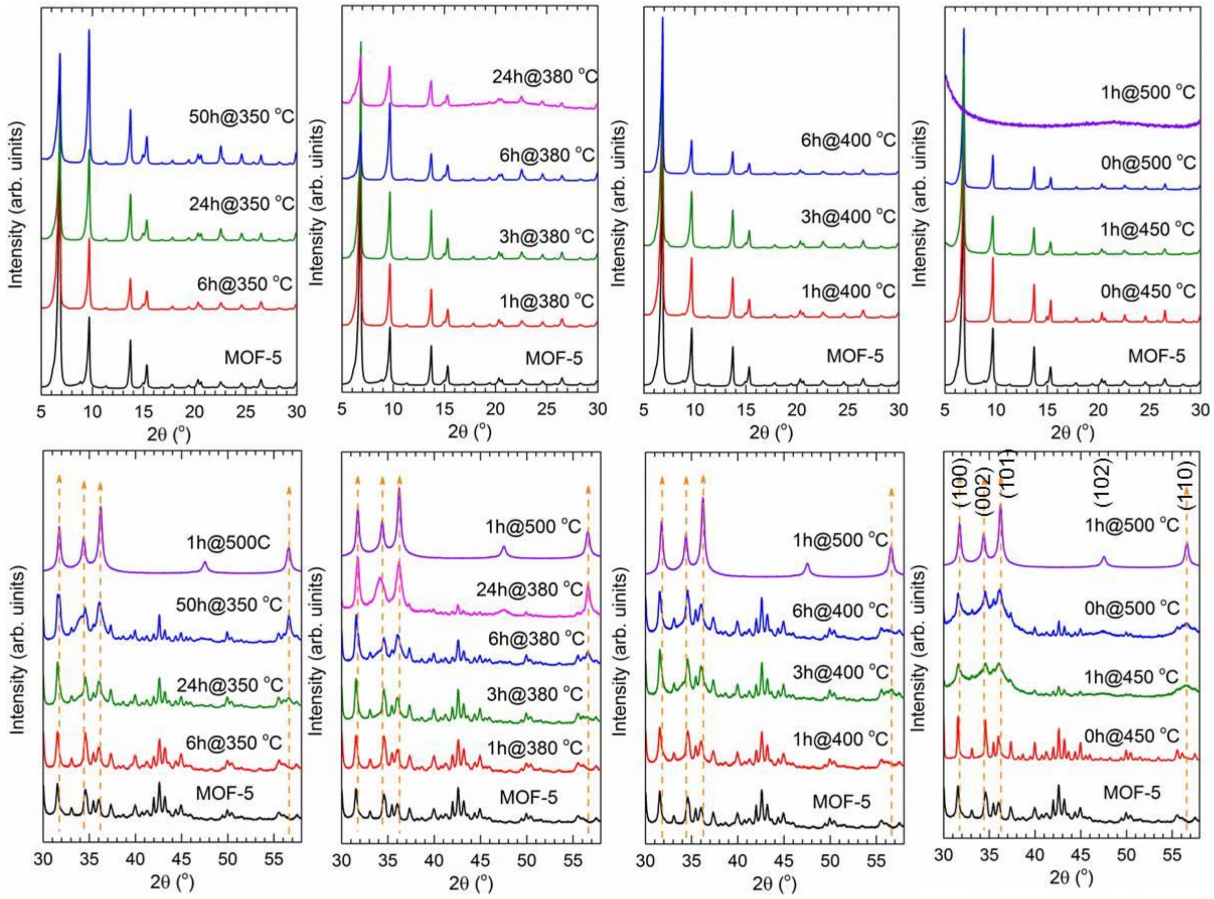

Figure S4. PXRD patterns of the MOF-5 and its annealed samples for different times and temperatures. Samples obtained at the same annealing temperature are grouped in one panel with MOF-5 as a reference. For clarity, top four panels show a low angle 2 theta data, and bottom four panels show high angle data to show ZnO formation. The vertical dashed arrows and asterisks represent the peaks from the hexagonal ZnO [see ref. 22, 27 in main text and Y. Lv, L. Yu, H. Huang, Y. Feng, D. Chen and X. Xie, Application of the soluble salt-assisted route to scalable synthesis of ZnO nanopowder with repeated photocatalytic activity, *Nanotechnology* 23 (2012) 065402].

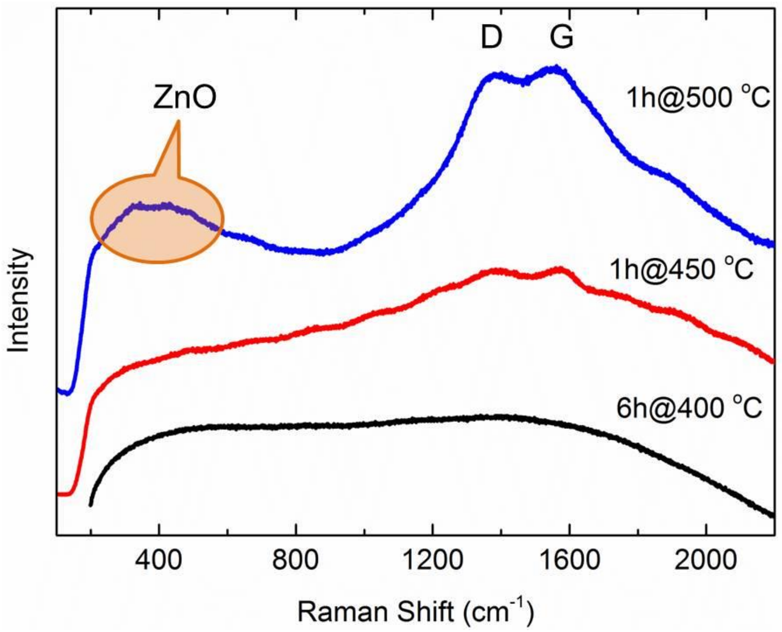

Figure S5. Raman spectra of annealed samples obtained at ≥ 400 °C showing a carbonization with the evidence of disordered carbon D and G bands at ~1380 cm^{-1} and ~1560 cm^{-1}, respectively. The ZnO formation is also seen by broad peak behaviour around 400 cm^{-1} [Ref. 35]. Due to the photoluminescence (PL) a dramatic change in the Raman spectra is observed in 6h@400 °C sample thus MOF-5 modes are totally overshadowed by the PL background [S. Bordiga, C. Lamberti, G. Ricchiardi, L. Regli, F. Bonino, A. Damin, K.-P. Lillerud, M. Bjorgen and A. Zecchina, Electronic and vibrational properties of a MOF-5 metal–organic framework: ZnO quantum dot behaviour, Chem. Commun., 2004, 2300–2301].

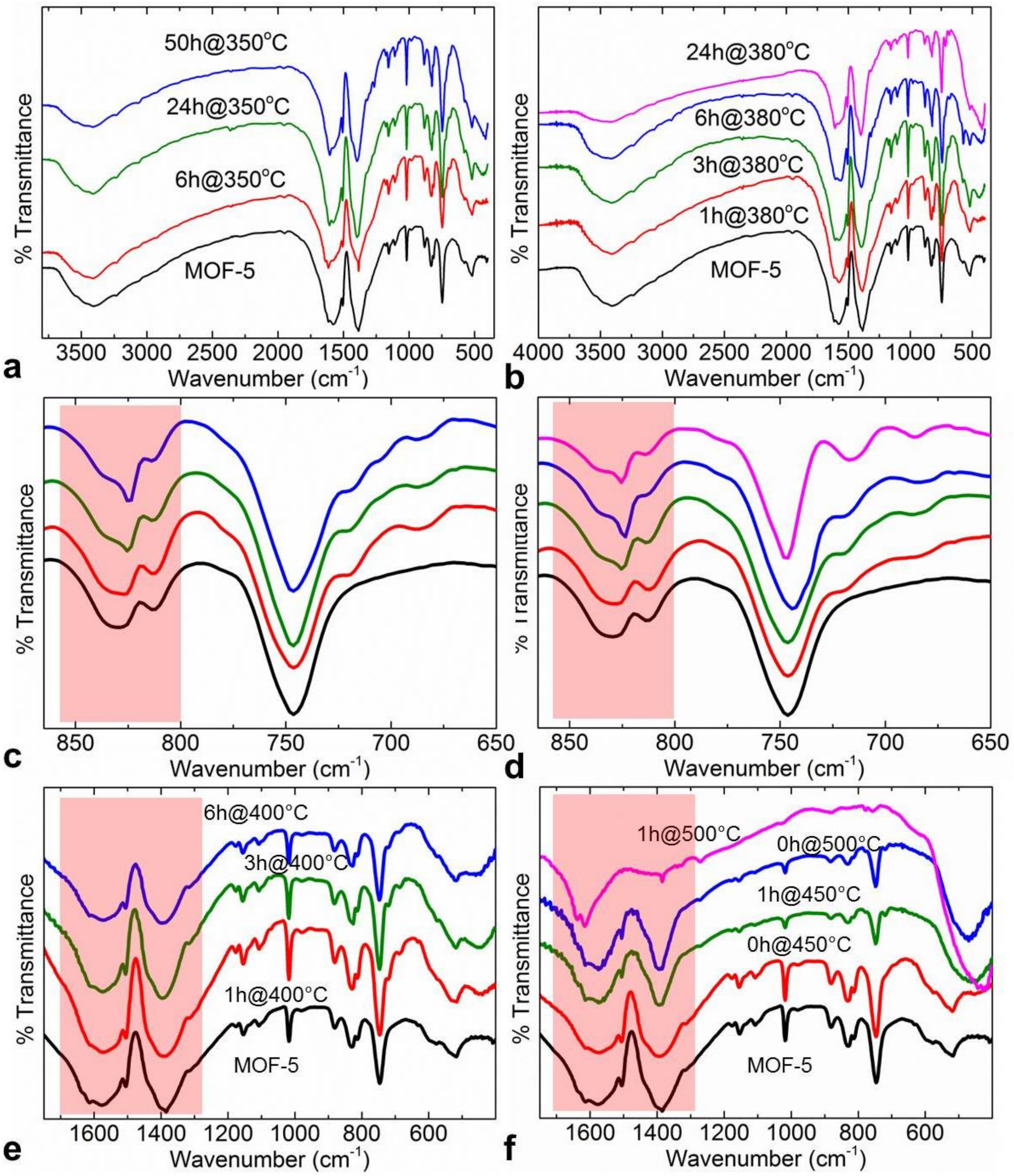

Figure S6. FTIR spectra of MOF-5 and its annealed samples [Ref. 36-39]; Full (a-b) and selected (c-d) range spectra for the annealed samples at (350-380) °C. e) and f) are for samples annealed at or above 400 °C. Clearly shows retention of all the framework IR modes in most of the annealed samples. IR bands in the region (1650–1300) cm^{-1} are assigned to asymmetric and symmetric modes of carboxylates, region (1300–600) cm^{-1} are assigned to the in-plane and out-of-plane deformation modes of aromatic ring, a band at 520 cm^{-1} is a characteristic Zn–O stretching vibration band of the tetrahedral coordinated Zn_4O cluster and broad band in the region (500–400) cm^{-1} is assigned to the Zn–O stretching in ZnO which is more prominent in the samples annealed at 450 °C and 500 °C. The highlighted regions show changes in carboxylate asymmetric and symmetric vibrations due to decarboxylation.

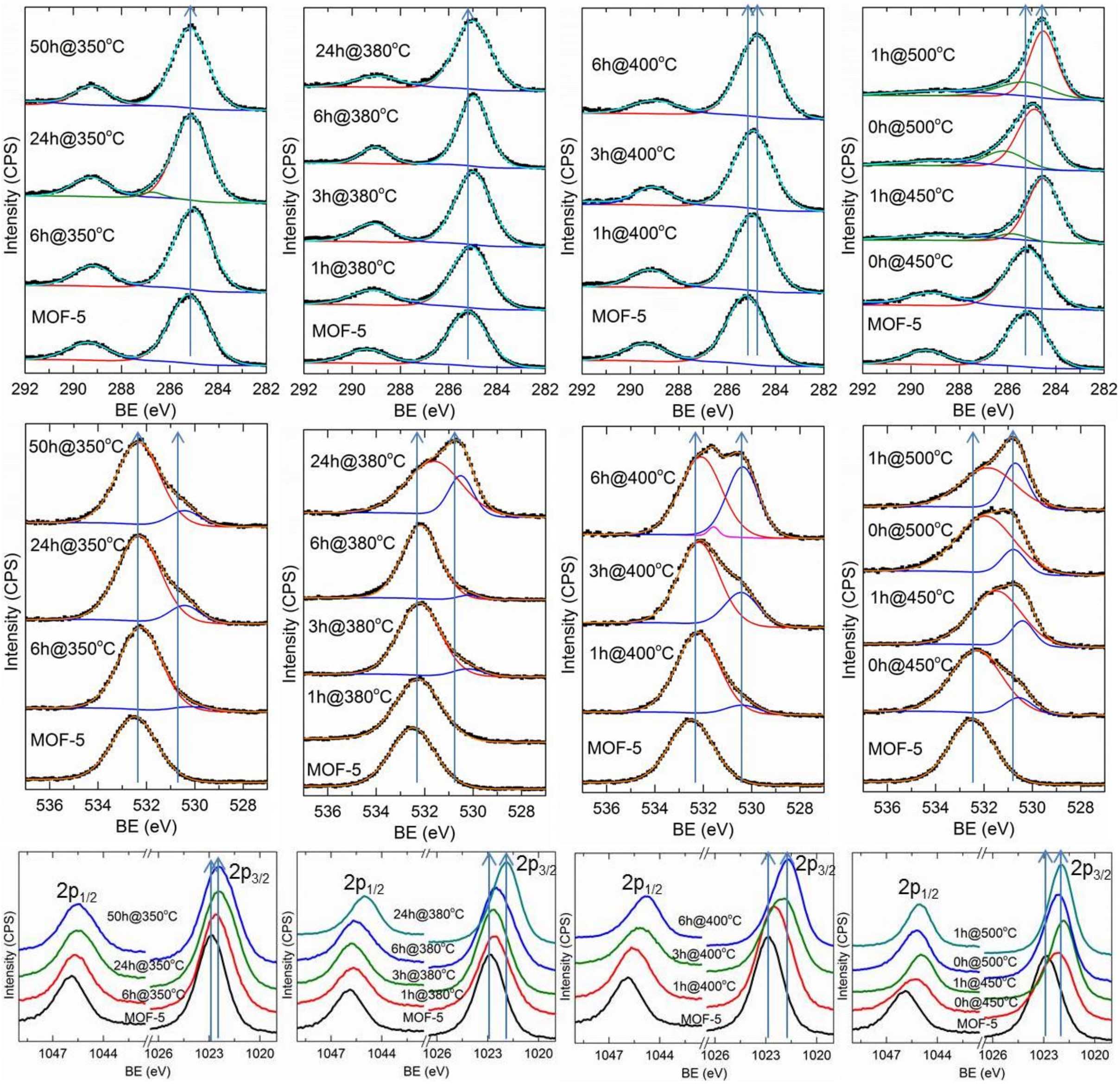

Figure S7. C 1s (top panel), O 1s (middle panel) and Zn 2p (bottom panel) core level XPS spectra of the MOF-5 and its annealed samples. Samples obtained at the same annealing temperature are grouped in one panel with MOF-5 as a reference. The vertical arrows show the respective peak potion, its relative shift and growing new peak corresponding to the ZnO formation [Ref. 22]. For the annealed samples, Zn $2p_{(3/2)}$ peak positions between MOF-5 (~1023 eV) and ZnO (~1022 eV) suggest a reduced Zn–O on linker coordination before turning into ZnO [Ref. 22,39]. The decomposition of carboxylates and formation of ZnO is clearly evidenced in O 1s peak splitting and growth of new peak at ~531 eV at the expense of actual carboxylate peak at ~532.5 eV.

By deconvolution of C 1s and O 1s peaks, the relative atomic percentage change in carboxylate sp^3 C to aromatic sp^2 C and O 1s carboxylate to ZnO is summarized in **Table S2**. As an example, O 1s peak accounts up to 10 % and maximum of 33 % conversion of oxygen to ZnO at mild and harsh annealing conditions, respectively. The CO_2 detected in TGA-MS due to decomposition of the linker carboxylates is also understood from the relative increase of sp^2 C percentage with respect to the carboxylate sp^3 C. Furthermore from **Table S2** it is conceivable that many bridged carboxylates remain intact in the annealed structures and thus show very good structural order of MOF-5, as evidenced by PXRD.

Table S2. XPS relative atomic % change (i.e., between sp^2 aromatic C to sp^3 carboxylate C and carboxylate O–Zn to ZnO) against annealing temperature and time.

Sample	C 1s		O 1s	
	sp^2 aromatic C	sp^3 carboxylate C	Zn–O on linker	ZnO conversion
MOF-5	77.8	22.2	100	0
6h@350°C	79.1	20.9	96.3	3.7
24h@350°C	79.5	20.5	87.4	12.6
50h@350°C	80.1	19.9	87.7	12.3
1h@380°C	77.9	22.1	98.3	1.7
3h@380°C	78.7	21.3	96.8	3.2
6h@380°C	80.4	19.6	93.3	6.7
24h@380°C	83.1	16.9	67.6	32.4
1h@400°C	79.9	20.1	91.7	8.3
3h@400°C	80.6	19.4	77.0	23.0
6h@400°C	83.5	16.5	67.7	32.3
0h@450°C	84.0	16.0	88.7	11.3
1h@450°C	90.0	10.0	82.5	17.5
0h@500°C	90.0	10.0	84.6	15.4
1h@500°C	98.0	2.0	66.8	33.2

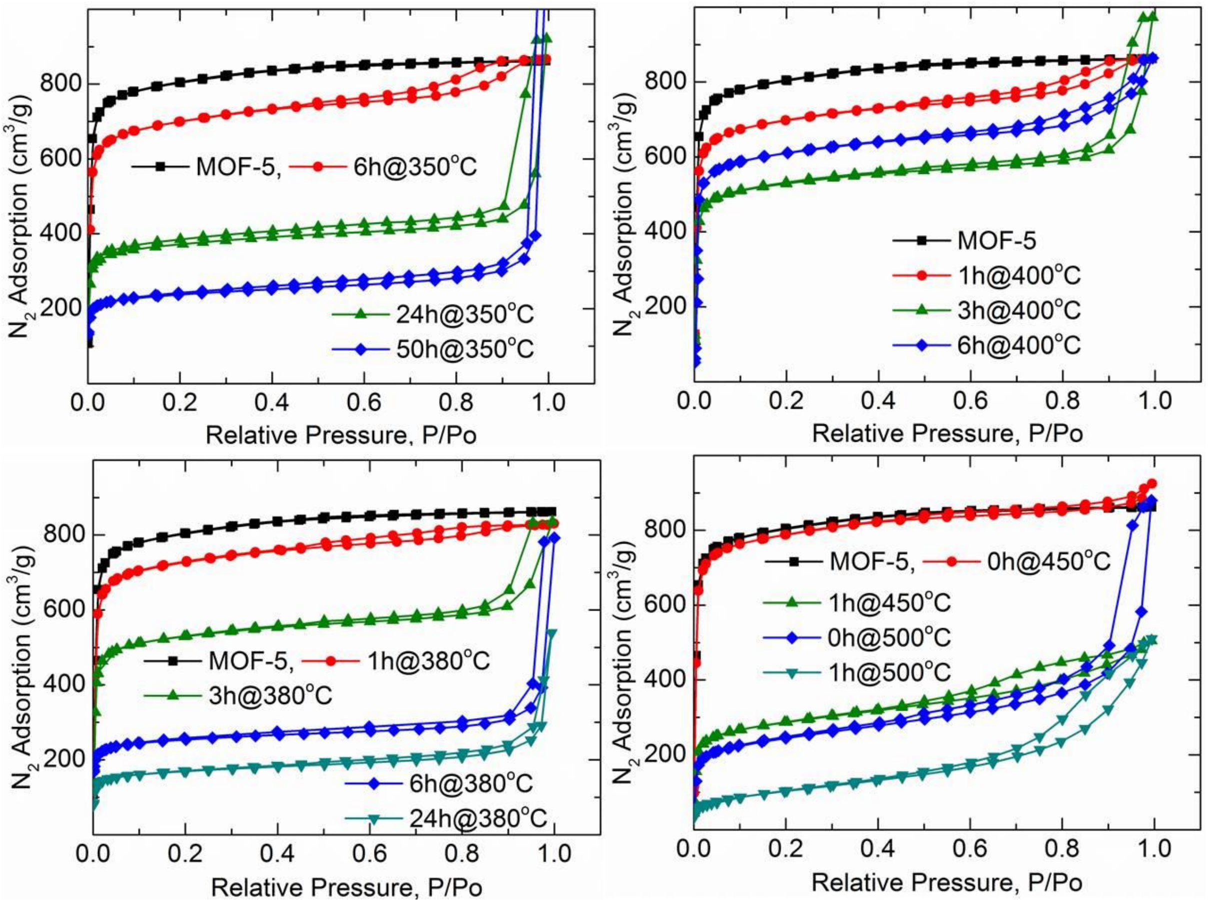

Figure S8. 77 K N_2 adsorption-desorption isotherms of all the annealed samples. Samples obtained at the same annealing temperature are grouped in one panel with MOF-5 as a reference, which is in good agreement with the literature [Ref. 1].

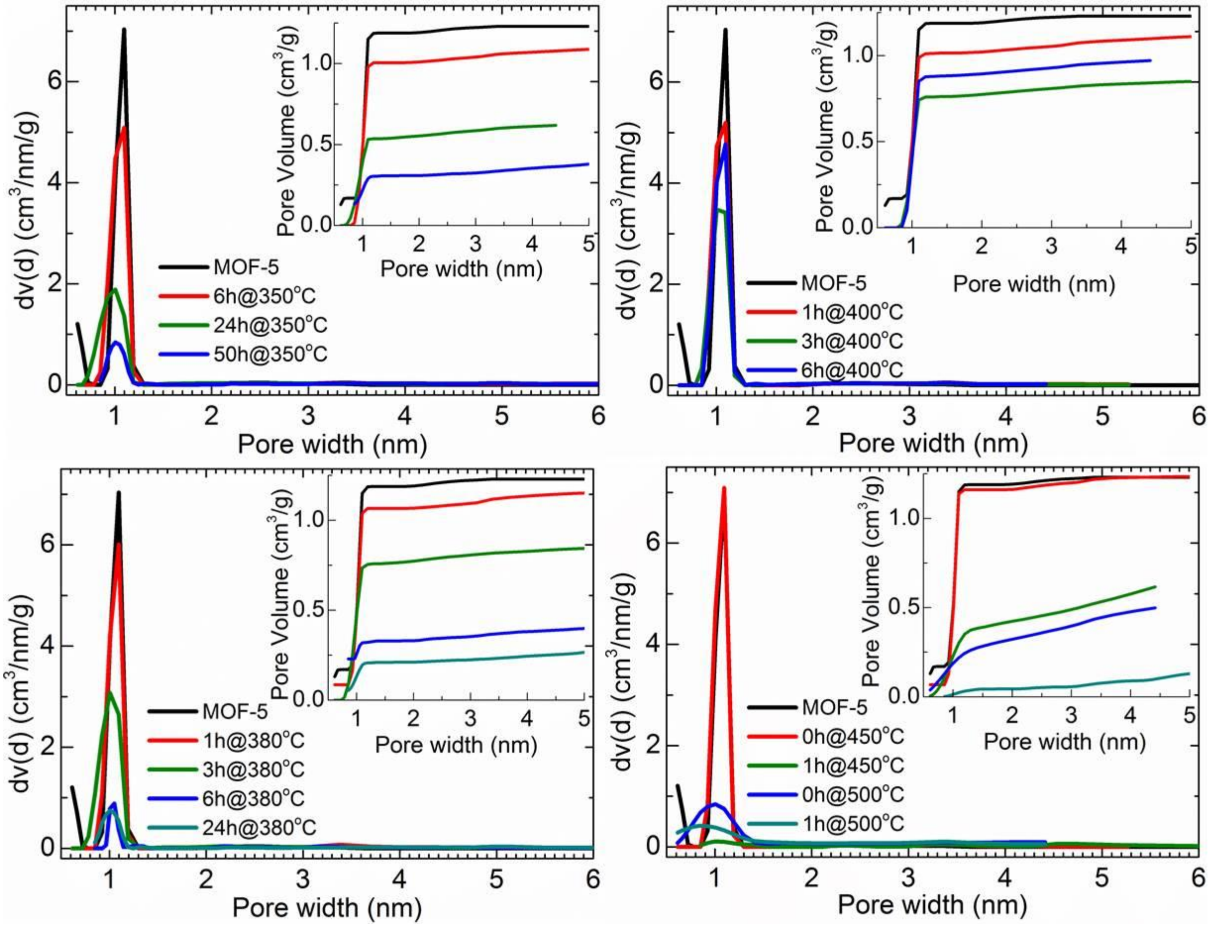

Figure S9. Pore size distribution and cumulative pore volume (insets) plots of all the annealed samples. Samples obtained at the same annealing temperature are grouped in one panel with MOF-5 as a reference.

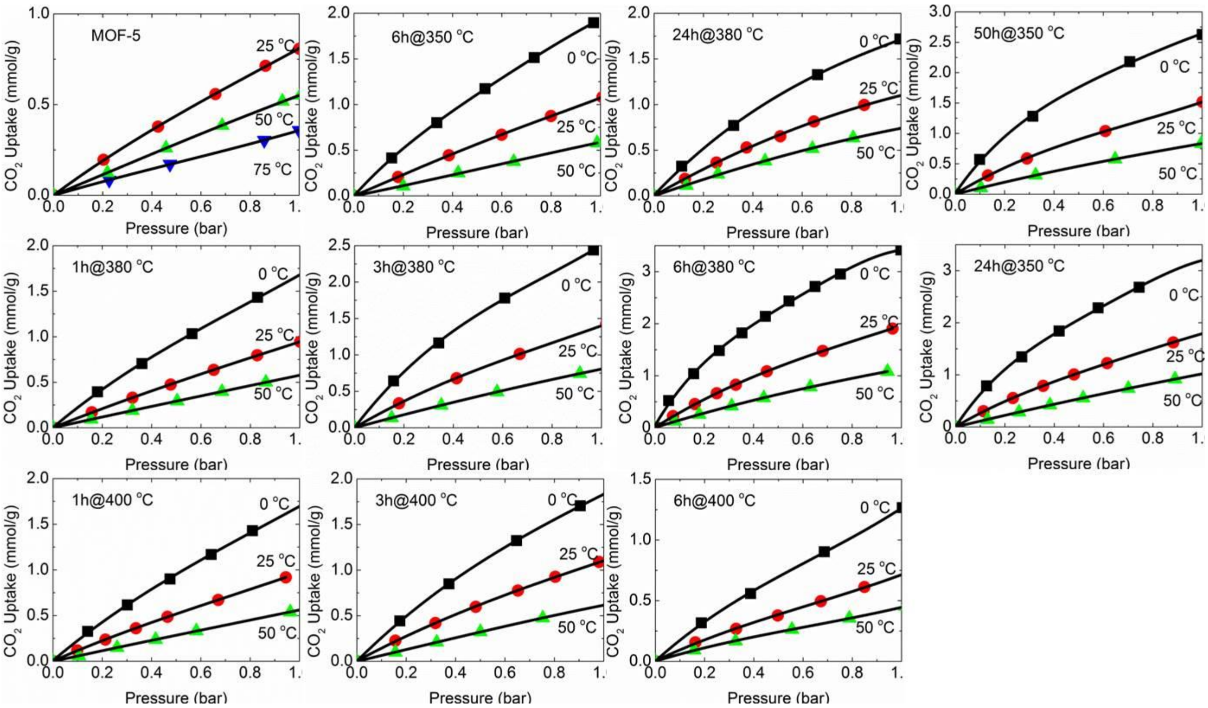

Figure S10. CO$_2$ uptake isotherms of all the annealed samples and MOF-5 (measured at three different temperatures; 0 °C, 25 °C and 50 °C for annealed samples and 25 °C, 50 °C and 75 °C for MOF-5). The solid data symbols are experimental data and continuous lines are from data polynomial fittings.

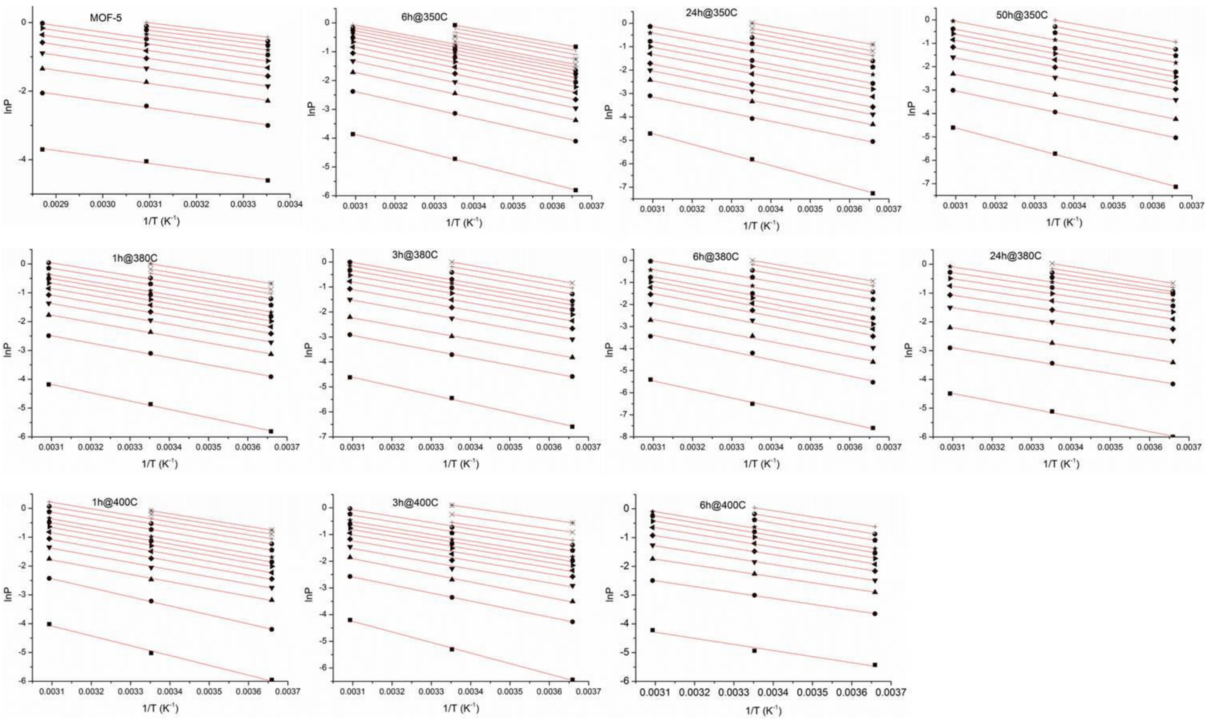

Figure S11. ln(P) vs 1/T plots for all the samples. Red lines are linear fittings to give slopes. The Q_{st} is obtained by applying Clausius-Clapeyron equation; simply $Q_{st} = -R \times (\text{Slope})$, where R is the universal gas constant.

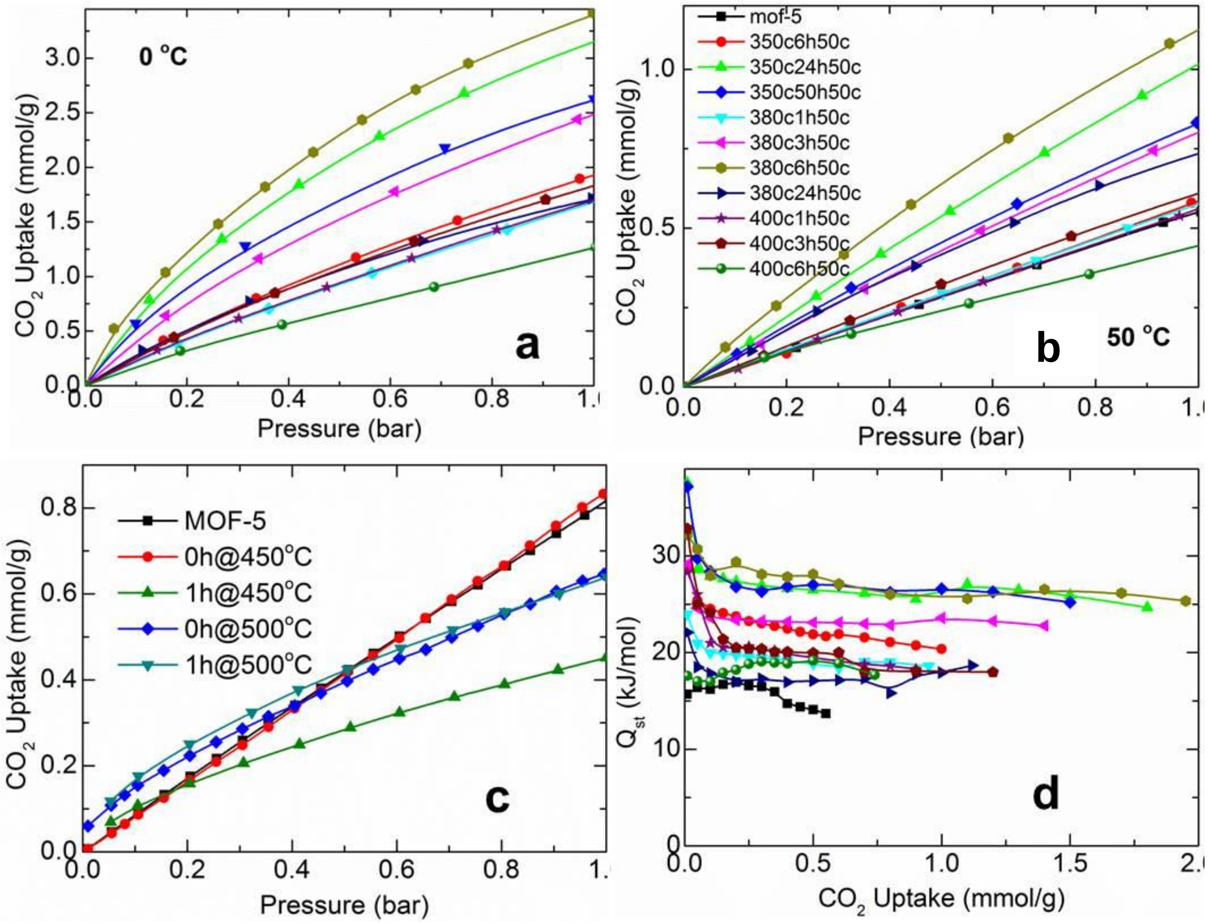

Figure S12. a-b). CO_2 uptake isotherms at 0 °C and 50 °C of the samples annealed between (350-400) °C. c). A comparative 25 °C CO_2 uptake isotherms of the MOF-5 and samples annealed at ≥ 450 °C or simply heated to (450-500) °C and cooled immediately.[see ref. 35] d). Q_{st} of MOF-5 and its annealed samples. The samples (a), (d) can be identified with the same colour code as labelled in 50 °C isotherm plot (b). Q_{st} in MOF-5 is in good agreement with the literature [Ref. 42]. Simultaneous carbonization and ZnO cluster formation in the samples obtained at harsh annealing conditions result in unfavourable CO_2 uptakes and binding with respect to the MOF-5. Thus the optimum conditions are 380 °C up to 6 h.

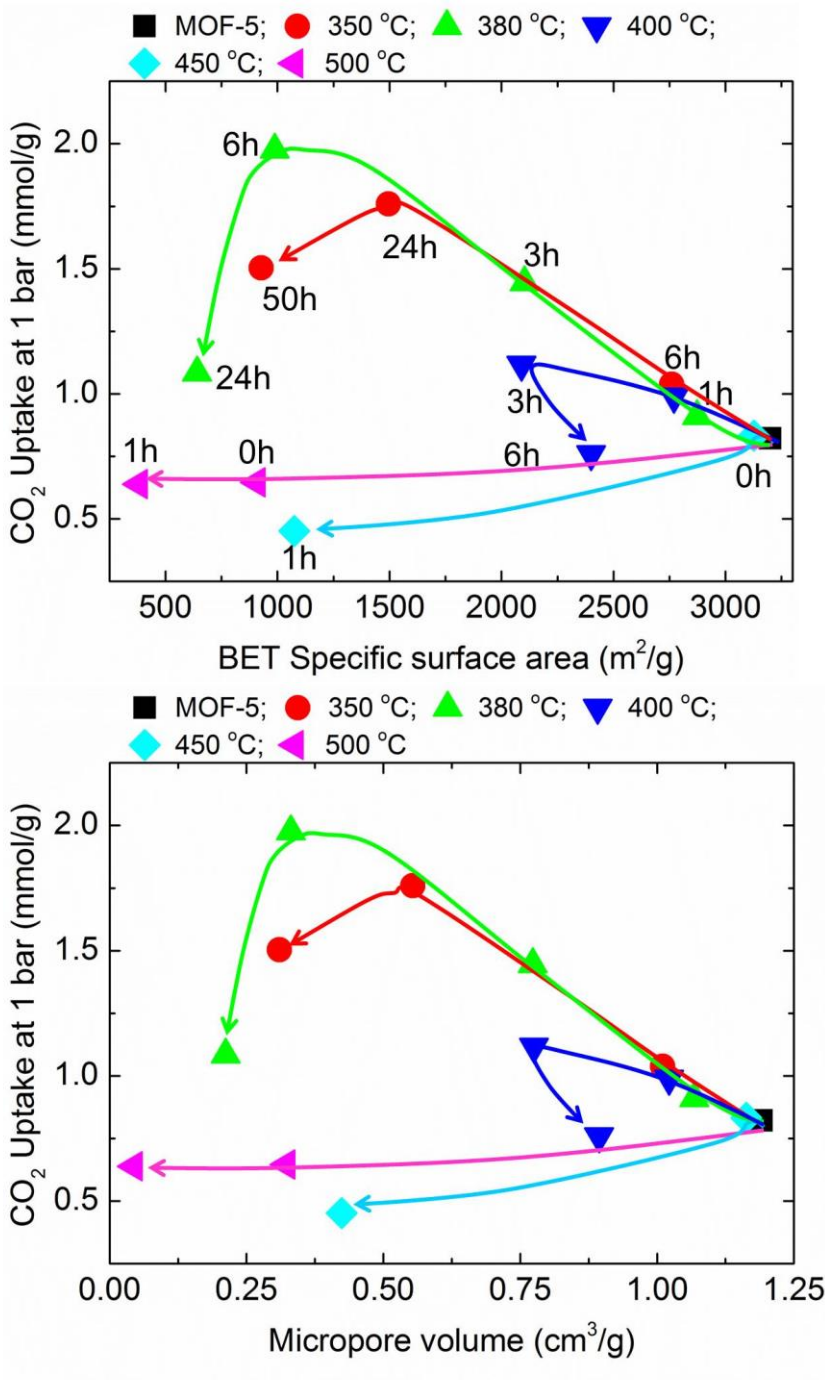

Figure S13. Variation of CO_2 uptake (at 1 bar and 25 °C) with respect to the increase in both the annealing temperature and time against BET surface area (top) and micropore volume (bottom). Arrow path shows the variation in uptake with respect to increased annealing period at same temperature. Clearly annealing at ≥ 400 °C is not effective in enhancing the uptake.

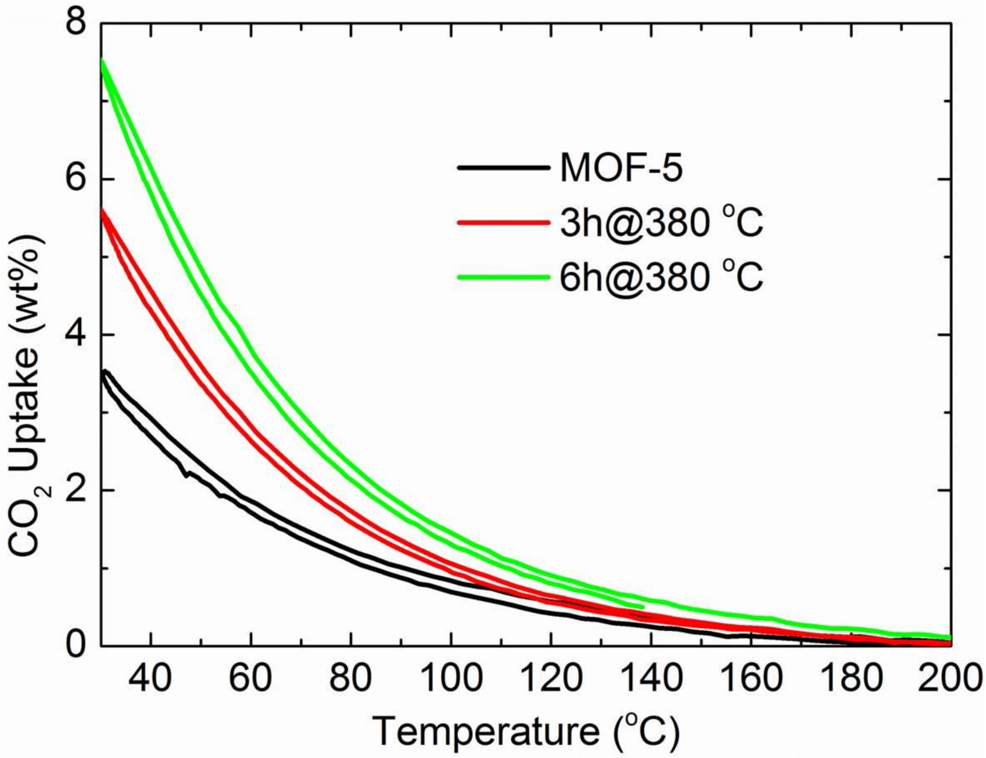

Figure S14. Variation of the TGA CO$_2$ uptake (in MOF-5 and sample annealed at 380 °C for 3 h and 6 h) under flowing CO$_2$ at ~1 atm against temperature swing between 31 °C and 200 °C with the heating rate of 10 °C per minute and natural TGA water cooling.

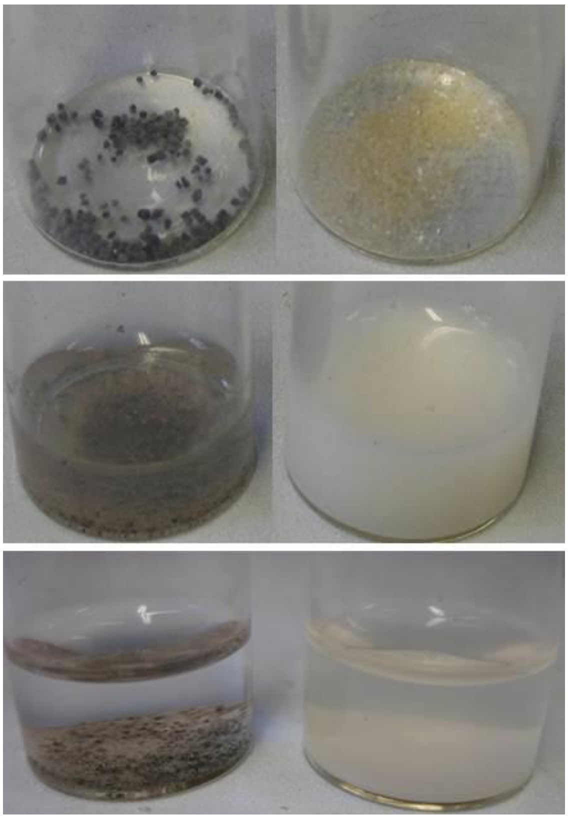

Figure S15. Digital photographs of annealed sample at 400 °C for 3 h (left) and MOF-5 (right): before being immersed in water (top), after adding deionised water (middle) and after 2 h in water (bottom).